

Long-tailed Recognition by Learning from Latent Categories

Weide Liu, Zhonghua Wu, Yiming Wang, Henghui Ding, Fayao Liu, Jie Lin and Guosheng Lin

Abstract—In this work, we address the challenging task of long-tailed image recognition. Previous long-tailed recognition methods commonly focus on the data augmentation or re-balancing strategy of the tail classes to give more attention to tail classes during the model training. However, due to the limited training images for tail classes, the diversity of tail class images is still restricted, which results in poor feature representations. In this work, we hypothesize that common latent features among the head and tail classes can be used to give better feature representation. Motivated by this, we introduce a Latent Categories based long-tail Recognition (LCReg) method. Specifically, we propose to learn a set of class-agnostic latent features shared among the head and tail classes. Then, we implicitly enrich the training sample diversity via applying semantic data augmentation to the latent features. Extensive experiments on five long-tailed image recognition datasets demonstrate that our proposed LCReg is able to significantly outperform previous methods and achieve state-of-the-art results.

Index Terms—Long-tailed recognition, Latent category.

I. INTRODUCTION

WITH the successful development of Convolution Neural Networks (CNNs), image recognition has achieved great success on the ideally collected balanced datasets (e.g., ImageNet [1] and Oxford Flowers-102 [2]). However, in most real-world applications, the natural image data often follows a long-tail distribution, where a few classes have abundant labeled images while most classes have only a few instances or a few annotations. The classification performance of the tail classes on such unbalanced datasets drops quickly with the conventional fully supervised training strategy.

Long-tailed image recognition has been proposed to address the imbalanced training data problem. The main challenges are

W. Liu is with School of Computer Science and Engineering, Nanyang Technological University (NTU), Singapore 639798 (e-mail: weide001@e.ntu.edu.sg).

Z. Wu is with School of Computer Science and Engineering, Nanyang Technological University (NTU), Singapore 639798 (e-mail: zhonghua001@e.ntu.edu.sg).

Y. Wang is with School of Computer Science and Engineering, Nanyang Technological University (NTU), Singapore 639798 (e-mail: yiming003@e.ntu.edu.sg).

H. Ding is with School of Electrical and Electronic Engineering, Nanyang Technological University (NTU), Singapore 639798 (e-mail: ding0093@e.ntu.edu.sg).

F. Liu is with the Institute for Infocomm Research (I²R)-Agency for Science, Technology and Research (A*star), Singapore, 138632 (e-mail: Liu_Fayao@i2r.a-star.edu.sg).

J. Lin is with the Institute for Infocomm Research (I²R)-Agency for Science, Technology and Research (A*star), Singapore, 138632 (e-mail: Lin-J@i2r.a-star.edu.sg).

G. Lin is with School of Computer Science and Engineering, Nanyang Technological University (NTU), Singapore 639798 (e-mail: gslin@ntu.edu.sg).

Corresponding author: Guosheng Lin.

W. Liu and Z. Wu make equal contributions.

the difficulties of handling the small-data learning problems and the extreme imbalanced classification over all the classes. Most of the long-tailed recognition methods [3]–[13] focus on generating more data samples of tail classes via data augmentation or using the re-balancing strategy to provide higher importance weights for the tail classes. For example, widely used data augmentation techniques like cropping, flipping, and mirroring are used to generate more data samples of the tail classes during the model training. However, we argue that the diversity of the training samples for the tail classes is still inherently limited due to the limited number of training images, which leads to subtle performance improvement for the long-tailed recognition task by using these conventional data augmentation methods.

Different from the conventional data augmentation methods, semantic data augmentation [14] tries to augment the image features by adding class-aware perturbations. The perturbations are sampled from the multivariate normal distribution, where the class-wise covariance matrices are calculated from all the training samples. However, directly applying semantic data augmentation to the long-tailed recognition task may not be optimal. This is because the calculated covariance matrix of the tail classes may not constitute satisfactory meaningful semantic directions for semantic augmentation due to the limited training samples. MetaSAug [15] tries to solve the imbalanced statistics problem by updating the class-wise covariance matrix by minimizing the LDAM loss on the validation sets. However, the performance is still constrained due to the limited diversity and training samples of the tail classes.

To overcome the limitations mentioned above, we propose to mine out and augment the common features among the head and tail classes to increase the diversity of the training samples. The commonality is obtained with the assumption that objects from the same domain might share some commonalities. For instance, cats and dogs share a commonality of legs with similar shapes and appearances. Motivated by this, we argue that it is feasible to re-represent the object features with the common features belonging to the ‘sub-categories’ i.e., each category contains parts of the target objects. For example, as shown in Figure 1, we can re-represent the dog and cat with a series of shared ‘sub-categories’ (e.g., head, leg, body, and tail) with different weights.

Specifically, we introduce a latent feature pool to store the common features, which can be learned through the back-propagation during the model training. As shown in Figure 2, the latent features from the pool are class-agnostic and shareable among all the classes. To ensure the latent features are meaningful and sufficient to represent object features, we

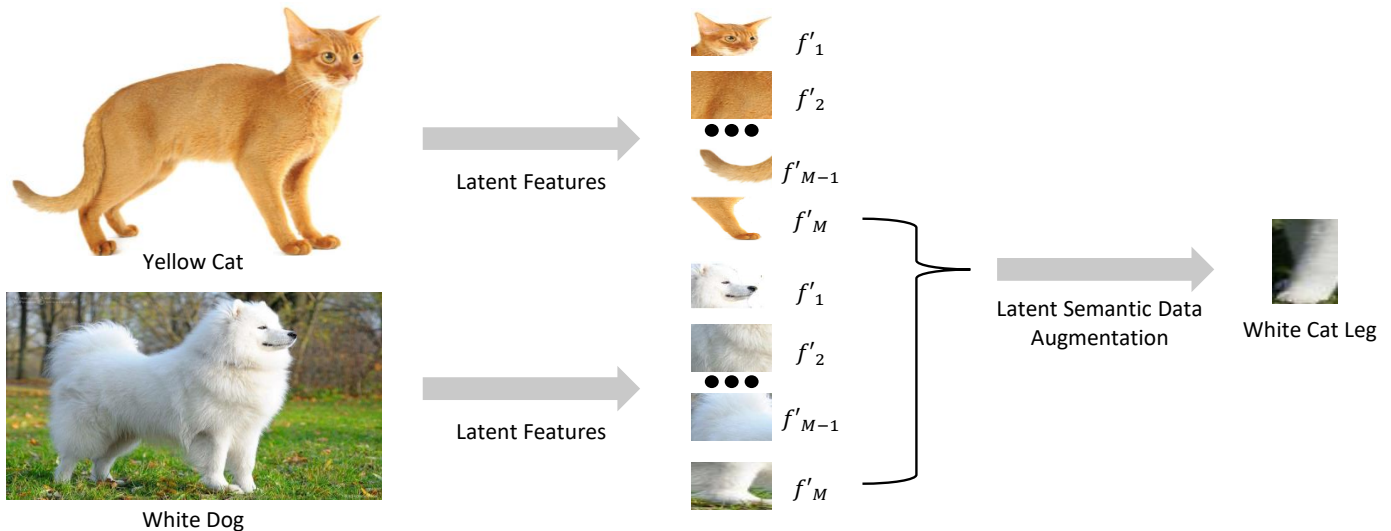


Fig. 1: Our LCRReg first projects the image features into the latent category features which share the commonality, such as the legs of cats and dogs. By performing the class semantic transformations along with the latent category, we aim to enrich the cat’s feature by leveraging the common features, e.g., change the yellow cat leg by leveraging the dog’s leg features.

apply a reconstruction loss to reconstruct the original object features with latent features. Each latent feature contributes to reconstructing the object with a similarity weight. Moreover, to further enrich the diversity of the training data, we implicitly apply a semantic data augmentation method to the latent feature pool. Our method has several advantages with the shareable latent features: 1) We transfer all the object features to the shareable latent categories, making the latent features class-agnostic, which allows our approach to no longer to be constrained to the imbalance distribution. This leads to 2) the tail class objects can benefit from the thriving diversity of the head with the shareable latent features. 3) The tail classes can benefit from the data augmentation technique with the increased diversity, which allows us to develop a latent semantic data augmentation in the latent space.

The main contributions of this work are concluded from three aspects:

- We design a Latent categories-based long-tail Recognition (LCRReg) method to address the training data imbalance problem. The proposed LCRReg explicitly learns the commonalities shared among the head and tail classes for better feature representations.
- We adopt a semantic data augmentation method on our proposed latent category features to implicitly enrich the diversity of the training samples.
- We conduct extensive experiments on multiple long-tailed recognition benchmark datasets (i.e., CIFAR-10-LT, CIFAR-100-LT, ImageNet-LT, iNaturalist 2018, and Places-LT) to validate the effectiveness of our LCRReg and achieve state-of-the-art performance.

II. RELATED WORK

A. Re-sampling and Re-weighting

With the successful development of Convolution Neural Networks (CNNs), image recognition [16]–[27] has achieved great success on the ideally collected balanced datasets. To deal with the unbalanced dataset, data re-sampling and loss re-weighting are common approaches for long-tailed recognition tasks. The core idea of data re-sampling is to forcibly re-balance the datasets by either under-sampling head classes [6], [7], [28] or over-sampling tail classes [7]–[9]. Likewise, loss re-weighting [3], [5], [29]–[31] approaches try to balance the loss of semantic classes according to their respective number of samples. However, these re-balancing approaches need careful calibration of weighting to prevent the training from overfitting to tail classes or underfitting to head classes. In particular, the data re-sampling approaches often result in insufficient training of head classes or overfitting to the tail classes; the loss re-weighting approaches suffer from unstable optimization during training [32]. In contrast to the re-sampling and re-weighting methods, our proposed LCRReg transfers the unbalanced object features to the shareable and balanced latent categories to learn the commonalities shared among the head and tail classes.

B. Decoupled Training

The decoupled training scheme [33] analyzes and finds that training with the entire long-tailed dataset is beneficial to the feature extractor but harmful to the classifier. Therefore, this two-stage approach proposes first to train the feature extractor and the classifier with the whole long-tailed datasets and then to finetune the classifier with the data re-sampling to balance the weight norm of each semantic class in the classifier. The

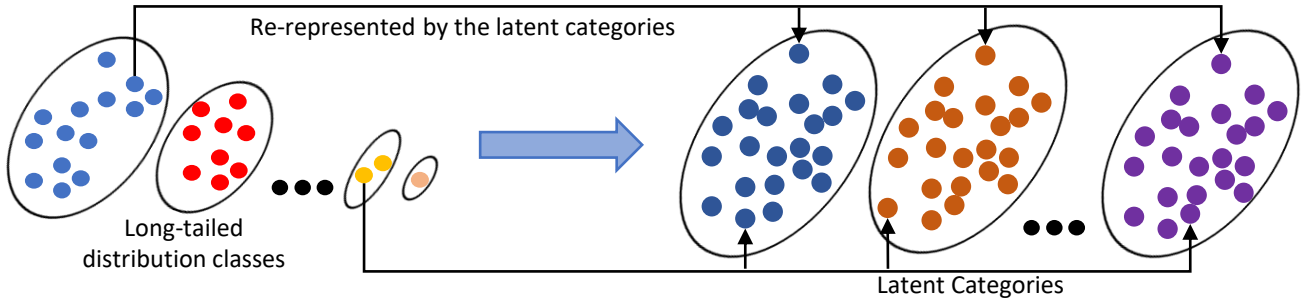


Fig. 2: Our LCRReg re-represent each object from the original long-tailed distribution dataset by the similarity-weighted sum of latent categories. The latent categories are shareable among the head and tailed classes and form a new balanced distributed dataset.

bilateral-branch network equivalently proposes the decoupled training scheme in the same period as [33] by adding an extra classifier for the finetuning such that the two-stage training becomes one. Besides the two-stage training scheme, a causal approach [34] proposes to learn the long-tail datasets in an end-to-end manner by removing the lousy momentum effect from the causal graph. As shown later, our proposed approach is also complementary to the decoupled training.

C. Data Augmentation

Data augmentation is another line of approaches to facilitate long-tailed recognition, as more augmented samples can alleviate the severely imbalanced distribution of datasets. Recent studies [32], [35], [36] demonstrate that the mixup helps the tail classes with enriched information from the head classes. Specifically, [32] additionally proposes label-aware smoothing for finetuning to boost the classification ability. Here, we take a step further to explore how the augmentation in the latent category space benefits the long-tailed classification. We follow another type of augmentation called semantic data augmentation [14] which has been explored recently in domain adaptation [37]. In long-tailed visual recognition, [15] proposes meta-learning to capture category-wise covariance for better augmentation. Unlike the existing augmentation approaches, we augment the latent category features through a latent semantic augmentation loss to diversify the training samples. We build our proposed method upon [32] to show that our method is also complementary to the data augmentation approaches.

III. METHOD

Given that a long-tail distributed dataset contains N training samples with C classes, we sample the i^{th} training sample x_i and its corresponding label y_i from the dataset. The final prediction for i^{th} sample \hat{y}_i is obtained from a classifier using the object feature $f_i \in \mathbb{R}^{D \times H \times W}$, which is generated by the encoder with parameters θ . Our training objective is to optimize the parameters θ and the classifier to minimize the distance between the prediction \hat{y}_i and the ground truth y_i . However, for long-tail distributed datasets, due to the imbalance distribution among each class, most of the features f_i are obtained from the head classes, which makes the

classification model biased toward the head classes, resulting in unsatisfactory performance on the tail classes. To alleviate the bias problem, we introduce a set of class-agnostic latent features f' , which store the common features among all the classes. In particular, each latent feature contributes to one part of the object features weighted by a similarity score. Moreover, we apply semantic data augmentation to the latent categories to further enrich the diversity of the training samples. The pipeline of our proposed LCRReg is shown in Figure 3.

A. Latent category features

Firstly, we introduce a set of shareable latent features $f'_0, f'_1, \dots, f'_m, \dots, f'_M$. Each latent feature depicts a latent category representing part of the object features, which is initialized by a random learnable embedding with a dimension of D and can be trained through back-propagation. The shape of each latent feature is $f'_m \in \mathbb{R}^{D \times 1}$, so all the latent feature shape is $\mathbb{R}^{D \times M}$.

We further calculate the similarity maps between latent features $f' \in \mathbb{R}^{D \times M}$ and image features $f \in \mathbb{R}^{D \times H \times W}$ from the image encoder, which benefits the following reconstruction process.

$$S^m = \sigma(\mathcal{FC}(f'_m)^T f), \quad (1)$$

where $S^m \in \mathbb{R}^{1 \times H \times W}$ indicates the m_{th} similarity map obtained by the m_{th} encoded latent feature $\mathcal{FC}(f'_m) \in \mathbb{R}^{D \times 1}$ and the image feature f . The \mathcal{FC} is a 1×1 convolutional layer to encode the latent features. We normalize the map with a Sigmoid function $\sigma(\cdot)$ and then reshape the similarity map.

B. Reconstruction Loss

To encourage the latent features containing more object information, we use the latent features to reconstruct the image features f by employing a reconstruction loss. Specifically, with the similarity maps $S \in \mathbb{R}^{M \times H \times W}$ generated by latent features, we apply a Softmax function over all the M similarity maps to identify the most discriminative object parts for each latent category $S^m \in \mathbb{R}^{1 \times H \times W}$:

$$\hat{S}^m = \frac{\exp(S^m)}{\sum_{k=1}^M \exp(S^k)}. \quad (2)$$

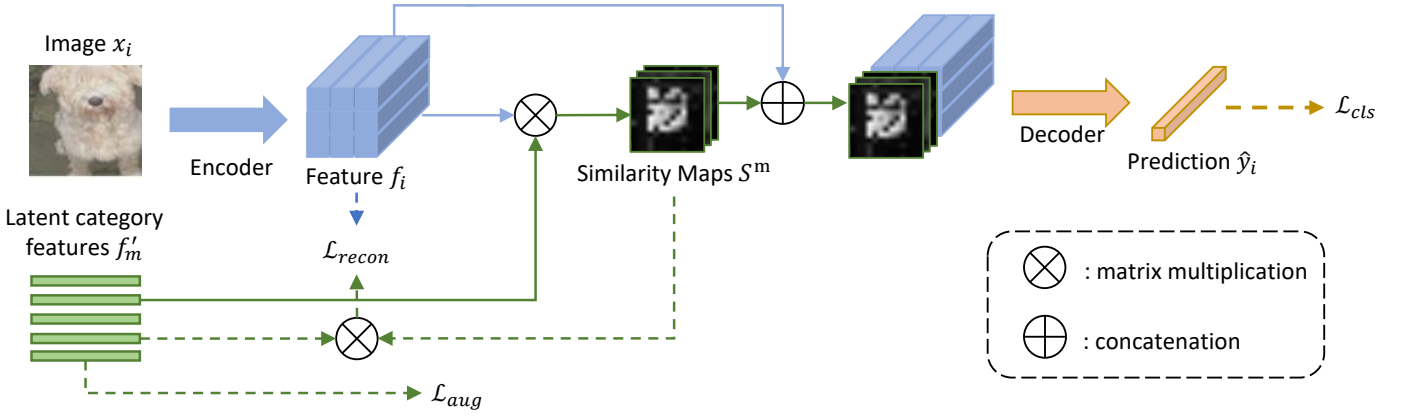


Fig. 3: The pipeline of our proposed LCReg.

Then we reconstruct image features f by summarizing all the latent categories with the weights from the normalized similarity maps:

$$\hat{f} = \sum_{m=1}^M \mathcal{F}\mathcal{C}(f'_m) \hat{S}^m. \quad (3)$$

To compare the reconstructed features $\hat{f} \in \mathbb{R}^{D \times HW}$ and the origin features $f \in \mathbb{R}^{D \times HW}$, we calculate the correlation matrix $C_f = \hat{f}^T f$, where $C_f \in \mathbb{R}^{HW \times HW}$ and H, W are the feature size. Finally, we employ a cross-entropy loss to maximize the log-likelihood of the diagonal elements of the correlation matrix $\text{diag}(C_f)$ to encourage each latent feature to learn distinct features:

$$\mathcal{L}_{Recon} = - \sum_{j=1}^{HW} t_j \log(\psi(\text{diag}(C_f))_j), \quad (4)$$

where j is the j^{th} diagonal element of the correlation matrix, and $t_j \in 1, 2, \dots, HW$ is the pseudo ground truth of the diagonal element, we define the first diagonal element of the correlation matrix $\text{diag}(C_f)$ to be the first category, the second one as the second category, and the rest in the same manner. The $\psi(\text{diag}(C_f))_j$ denotes the Softmax probability for the j^{th} category.

C. Latent Feature Augmentation

Data augmentation is a powerful technique that has been widely used in recognition tasks to increase training samples to reduce the over-fitting problem. Traditional data augmentation, such as rotation, flipping, and color-changing, are utilized to increase the training samples by changing the image itself. In contrast to conventional data augmentation techniques, semantic data augmentation augments the semantic features by adding class-wise conditional perturbations [14]. The performance of such class-conditional semantic augmentation heavily relies on the diversity of the training samples to calculate significant, meaningful co-variance matrices for perturbation sampling. However, in the long-tail recognition task, the diversity of tail classes is low due to the limited

training samples. The calculated class-conditional statistics will not include sufficient meaningful semantic direction for feature augmentation, which causes negative effects on long-tailed recognition tasks. The details are shown in Section IV-D and Table IV.

Latent implicit semantic data augmentation. In contrast with ISDA [14], we propose to augment the latent categories to implicitly generate more training samples. To implement the semantic augmentation in the latent feature categories directly, we calculate the co-variance matrices ($\Sigma = \{\Sigma_1, \Sigma_2, \dots, \Sigma_M\}$) for each latent category by updating the latent features f'_m at each iteration over total M classes. In particular, for the t^{th} training iteration, we have total $n_m^{(t)} = n_m^{(t-1)} + n_m^{\prime(t)}$ training samples for m_{th} latent category, where the $n_m^{\prime(t)}$ denotes the number of training samples at the current t^{th} iteration for m_{th} latent category. Then we estimate the average latent feature value $\mu_m^{(t)}$ of m_{th} latent category for total t iteration with:

$$\mu_m^{(t)} = \frac{n_m^{(t-1)} \mu_m^{(t-1)} + n_m^{\prime(t)} \mu_m^{\prime(t)}}{n_m^{(t)}}, \quad (5)$$

where the $\mu_m^{\prime(t)} = \frac{1}{n_m^{\prime(t)}} \sum_1^{n_m^{\prime(t)}} f'_m$ denotes the current average values of the latent m_{th} class features at t^{th} iteration. Then we can update the m_{th} latent category covariance matrices for total t training iteration with:

$$\Sigma_m^{(t)} = \frac{n_m^{(t-1)} \Sigma_m^{(t-1)} + n_m^{\prime(t)} \Sigma_m^{\prime(t)}}{n_m^{(t)}} + \frac{n_m^{(t-1)} n_m^{\prime(t)} \Delta(\mu) \Delta(\mu)^T}{(n_m^{(t)})^2}, \quad (6)$$

where $\Delta(\mu) = (\mu_m^{(t-1)} - \mu_m^{\prime(t)})$, and the $\Sigma_m^{\prime(t)}$ denotes the m_{th} latent category covariance matrices at current t^{th} iteration.

Then, we augment the features by sampling a semantic transformation perturbation from a Gaussian distribution $\mathcal{N}(0, \lambda \Sigma_{y'_m})$, where λ indicates the hyperparameter of the augmentation strength and $y'_m \in 1, \dots, M$ indicates the pseudo ground truth of the M latent categories. In particular, we set

Dataset	Methods	Many	Medium	Few
CIFAR10-LT IF 100	Ours*	90.9	80.8	73.7
	Ours	92.6	81.5	75.4
CIFAR100-LT IF 100	OLTR [38]	61.8	41.4	17.6
	LDAM + DRW [39]	61.5	41.7	20.2
	τ -norm [33]	65.7	43.6	17.3
	cRT [33]	64.0	44.8	18.1
	Ours*	63.1	48.4	25.3
	Ours	64.2	49.2	25.3
ImageNet-LT	cRT [33]	62.5	47.4	29.5
	LWS [33]	61.8	48.6	33.5
	Ours*	61.7	51.3	35.8
	Ours	66.2	52.9	35.8
iNaturalist 2018	cRT [33]	73.2	68.8	66.1
	τ -norm [33]	71.1	68.9	69.3
	LWS [33]	71.0	69.8	68.8
	Ours*	73.2	72.4	70.4
	Ours	73.8	73.4	71.5

TABLE I: We report accuracy on three splits of classes: Many, Medium, and Few. We validate our methods on multiple datasets, including small-scale datasets (CIFAR10-LT, CIFAR100-LT with IF 100) and large-scale datasets (ImageNet-LT, and iNaturalist 2018). Ours* indicates ours baseline (without the latent category features, reconstruction loss \mathcal{L}_{Recon} and latent augmentation loss \mathcal{L}_{latent_aug}).

Dataset	Number of latent class					Dataset	Number of latent class			
	20	30	40	50	60		20	60	100	200
CIFAR-10-LT	81.9	82.4	83.1	82.5	79.6	ImageNet-LT	54.5	55.0	55.3	55.2
CIFAR-100-LT	47.1	47.2	47.4	47.6	46.1	iNaturalist 2018	-	71.6	71.6	72.6

TABLE II: Ablation studies of the effectiveness of the number of latent categories. We conduct the experiments on the small dataset (CIFAR-10-LT and CIFAR-100-LT with IF 100) and large dataset (ImageNet-LT and iNaturalist 2018). The larger the dataset (more training samples and classes), the more latent categories are needed to represent better performances.

Components			CIFAR-10-LT			CIFAR-100-LT			iNaturalist 2018
latent category	latent aug	latent recon	100	50	10	100	50	10	-
			82.1	85.7	90.0	47.0	52.3	63.2	68.9
✓			82.2	85.8	90.7	47.2	52.6	63.9	69.4
✓	✓		82.5	86.0	91.0	47.4	53.0	64.1	69.8
✓		✓	83.0	86.2	91.1	47.3	52.5	64.0	70.0
✓	✓	✓	83.1	86.5	91.2	47.6	53.1	64.2	70.5

TABLE III: Ablation studies of each component, including whether utilizing our proposed latent category, latent augmentation loss(latent aug) and latent reconstruction loss (latent recon). We conduct the experiments on the small dataset (CIFAR-10-LT and CIFAR-100-LT with IF 100, 50, and 10) and large dataset (iNaturalist 2018). The results show that each of our proposed components improves the baseline (without any component).

the first latent category as the first class, the second one as the second class, and the rest in the same manner. For each augmented latent feature f_m^a we have

$$f_m^a \sim \mathcal{N}(f_m', \lambda \Sigma_{y_m'}). \quad (7)$$

Furthermore, when we sample infinite times to explore all the possible meaningful perturbations in the $\mathcal{N}(0, \lambda \Sigma_{y_m'})$, there is an upper bound of the cross-entropy loss [14] on all

the augmented features over N training samples:

$$\begin{aligned} \mathcal{L}_{latent_aug} &= \sum_{i=1}^N L_{\infty}(f(\mathbf{x}_i; \theta), y_m'; \Sigma) \\ &= \frac{1}{N} \sum_{i=1}^N \log \left(\sum_{j=1}^M e^{z_j} \right) \end{aligned} \quad (8)$$

$$\begin{aligned} z_j &= (w_j^T - w_{y_m'}^T) f_m^a + (b_j - b_{y_m'}) + \\ &\quad \frac{\lambda}{2} (w_j^T - w_{y_m'}^T) \Sigma_{y_m'} (w_j - w_{y_m'}), \end{aligned} \quad (9)$$

Methods	CIFAR-10-LT			CIFAR-100-LT		
	100	50	10	100	50	10
Baseline	82.1	85.7	90.0	47.0	52.3	63.2
+ ISDA	79.8	82.7	87.8	43.5	47.8	57.7
+ L_{Aug}	82.5	86.0	91.0	47.4	53.0	64.1

TABLE IV: Ablation studies for the normal feature augmentation with ISDA and the latent feature augmentation. L_{Aug} denotes the method applying the latent augmentation method on the latent category features. We report the top-1 accuracy (%) on different datasets.

Method	CIFAR-10-LT			CIFAR-100-LT		
	100	50	10	100	50	10
CE (Cross Entropy)	70.4	74.8	86.4	38.4	43.9	55.8
mixup [40]	73.1	77.8	87.1	39.6	45.0	58.2
LDAM+DRW [41]	77.1	81.1	88.4	42.1	46.7	58.8
BBN(include mixup) [35]	79.9	82.2	88.4	42.6	47.1	59.2
Remix+DRW [42]	79.8	-	89.1	46.8	-	61.3
MiSLAS [32]	82.1	85.7	90.0	47.0	52.3	63.2
MetaSAug CE [15]	80.5	84.0	89.4	46.9	51.9	61.7
Ours	83.1	86.5	91.2	47.6	53.1	64.2

TABLE V: Top-1 accuracy (%) for ResNet-32 based models trained on CIFAR-10-LT and CIFAR-100-LT.

where θ indicates the encoder parameters for the latent category features. w and b are the weight and biases corresponding to the 1×1 convolution layer \mathcal{FC} mentioned above. Following ISDA [14], we let $\lambda = (t/T) \times \lambda_0$ to reduce the augmentation impact in the beginning of the training stage, where T indicates the total iteration.

With the augmented latent category features, we are able to increase the diversity of training samples by reconstructing the augmented latent features back to the image features f with the reconstruction loss \mathcal{L}_{Recon} .

D. Training Process

We adopt decoupled training for the long-tailed task as in [32]. Specifically, in the first stage of the training process, our training objective includes the reconstruction loss \mathcal{L}_{Recon} which is applied on the latent category features, a latent augmentation loss \mathcal{L}_{latent_aug} that augments the latent features, and a cross-entropy classification loss which is applied on final prediction \hat{y}_i generated with the decoder. We optimize the network parameter by combining all the losses:

$$\mathcal{L} = \alpha \mathcal{L}_{latent_aug} + \beta \mathcal{L}_{Recon} + \gamma \mathcal{L}_{cls}, \quad (10)$$

where L_{cls} indicates the final classification loss (CE loss) between the ground truth y and the prediction \hat{y}_i . α , β , and γ are the trade-off parameters, which have been set to 0.1, 0.1 and 1, respectively. In the second stage of training, following [32], we finetune the network.

IV. EXPERIMENTS

A. Implementation Details

We follow the training pipeline as in [32], [35] to conduct experiments on five datasets, including CIFAR-10-LT, CIFAR-100-LT, ImageNet-LT, iNaturalist 2018, and Places-LT. We

Method	ResNet-50
CE	44.6
CE+DRW [41]	48.5
Focal+DRW [43]	47.9
LDAM+DRW [41]	48.8
NCM [33]	44.3
τ -norm [33]	46.7
cRT [33]	47.3
LWS [33]	47.7
MiSLAS [32]	52.7
MetaSAug CE [15]	47.4
Ours	55.3

TABLE VI: Top-1 accuracy (%) on ImageNet-LT.

Method	ResNet-50
CB-Focal [44]	61.1
LDAM+DRW [41]	68.0
OLTR [38]	63.9
cRT [33]	65.2
τ -norm [33]	65.6
LWS [33]	65.9
BBN(include mixup) [35]	69.6
Remix+DRW [42]	70.5
MiSLAS [32]	71.6
MetaSAug CE [15]	68.8
Ours	72.6

TABLE VII: Top-1 accuracy (%) on iNaturalist 2018.

use the SGD as the optimizer to train the network. We apply data augmentation such as random scale, random crop, and random flip during the training process. If there is no special declaration, we conduct the experiments with a batch size of 128.

B. Dataset

CIFAR-10-LT and CIFAR-100-LT. Following [39], we conduct experiments on the long-tail version of CIFAR datasets. CIFAR-10 and CIFAR-100 contain 50000 images and 10000 for training and validation, including 10 and 100 categories, respectively. In particular, we discard the training samples to reorganize a unbalanced dataset with imbalance factor(IF) $\beta = N_{max}/N_{min}$. The N_{max} and N_{min} are the numbers of training samples for the largest and the smallest classes. Following [32], [35], [39], we conduct the experiments on the CIFAR-LT with imbalance factor(IF) $\beta = 10, 50$ and 100.

ImageNet-LT. Liu *et al.* [38] propose the ImageNet-LT dataset, which contains 115,846 training images and 50,000 validation images, including 1000 categories, with the imbalance factor(IF) of 1280/5. This dataset is a subset of ImageNet [1]. They follow the Pareto distribution with power value $\alpha = 6$ to sample the images and rearrange to a new unbalanced dataset.

iNaturalist 2018. iNaturalist 2018 [48] is a large-scale dataset collected from the real world, whose distribution is extremely unbalanced. It contains 435,713 images for 8142 categories with imbalanced factor(IF) of 1000/2.

Places-LT. Places-LT is a long-tailed distribution dataset generated from the large-scale scene classification dataset

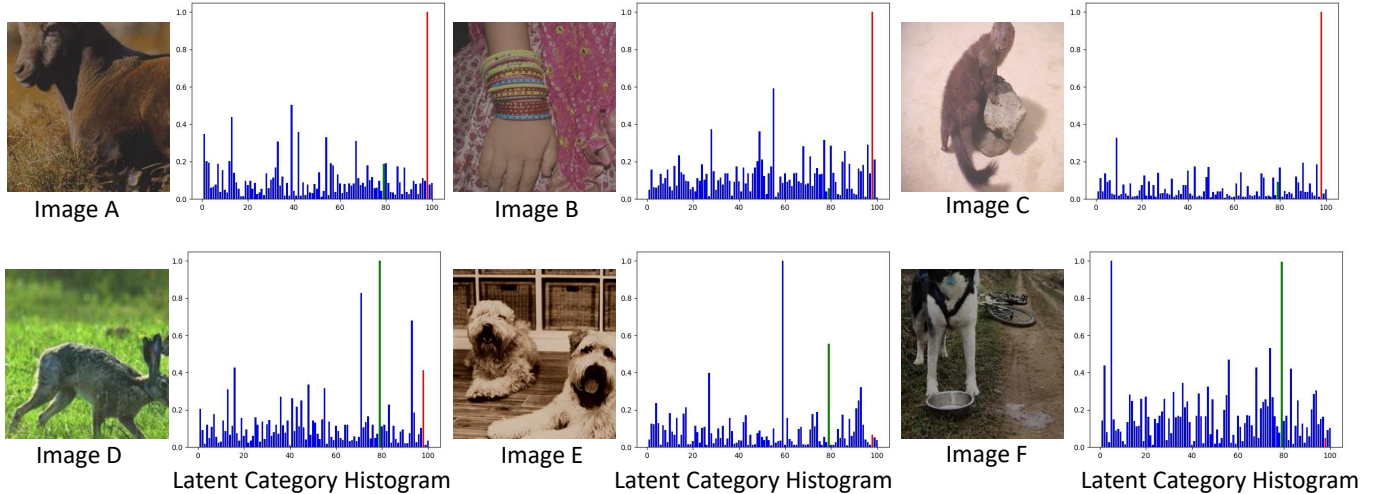


Fig. 4: We visualize the weight histogram of latent categories contributing to the reconstruction of the image features. As shown in the figures, the 79th latent category (green) is highlighted by the ‘hare’(Image D), and ‘dogs’(Image E and F), while all of them contain the similar shape of the limbs. Furthermore, the ‘cow’(Image A), ‘human arm’(Image B), and ‘fisher’(Image C) share some commonalities captured by the 98th latent category(red). Note that our proposed method aims to learn some commonalities between images belonging to latent classes. The latent classes are not only denoted for the appearances from the human point of view. A common characteristic can be any characteristic of an object, such as color, structure, or shape.

Method	ResNet-152
Range Loss [45]	35.1
FSLwF [46]	34.9
OLTR [38]	35.9
OLTR+LFME [47]	36.2
Ours	40.2

TABLE VIII: Top-1 accuracy (%) on Places-LT.

Places [49]. It consists of 184.5K images for 365 categories with an imbalanced factor(IF) of 4980/5.

C. Comparisons with State-of-the-art methods

Experiments on CIFAR-LT. Following [32], [34], [35], [41], we conduct the experiments on CIFAR-10-LT and CIFAR-100-LT with the IF of 10, 50, and 100. The latent categories are set to 40 and 50 for CIFAR-10-LT and CIFAR-100-LT, respectively. As shown in Table V, our proposed method outperforms all previous methods.

Experiments on large-scale datasets. We further validate the effectiveness of our method on the large-scale imbalanced datasets, *i.e.*, ImageNet-LT, iNaturalist 2018, and Places-LT. The latent category number is set to 100 for ImageNet-LT and 200 for iNaturalist 2018, and 100 for the Places-LT dataset. As shown in Table VI, Table VII and Table VIII, our proposed method outperforms all the other methods and achieves the new state-of-the-art performance on all the large-scale datasets.

D. Ablation Studies

Number of the latent categories. We conduct experiments to analyze how the latent categories affect the performance of different datasets. As shown in Table II, we experiment on

both small and large scale datasets to explore the effectiveness of the number of latent categories. For the larger datasets, which contain more training samples and classes, we suggest using more latent categories to represent the original image features to achieve better performances. However, enlarging the number of latent categories could not continuously increase the performances. For example, 40 categories yield the best performance on the CIFAR-10-LT dataset. Continually increasing the number of categories would drop the performances very quickly. We speculate that if there are too many latent categories, each object feature might be split too finely by the latent features, failing to obtain the meaningful parts.

Performance on different splits of classes. We further report the classification accuracy for the many (more than 100 images per class), medium (20 to 100 images per class), and the few (less than 20 images per class) classes. In particular, we set the number of latent categories as 40 for CIFAR-10-LT, 50 for CIFAR-100-LT, 100 for ImageNet-LT, and 200 for iNaturalist 2018. As shown in Table I, our method achieves the best performance on the many, medium, and few classes by a large margin for all the datasets. Specifically, on the ImageNet-LT ‘many’ dataset, our LCReg achieves a 4.4% accuracy gain over the previous SOTA methods while keeping the performances of medium and few classes not dropped.

Effect of each component. We investigate the contribution of each component of our proposed method: the latent categories, the latent augmentation loss, and the latent reconstruction loss. We conduct the ablation experiments on both the small and large scale datasets to validate our method. Specifically, we choose the imbalance factor(IF) to 100 and set the number of latent categories to 40 for CIFAR-10-LT and 50 for CIFAR-100-LT. For the experiment on the large challenge datasets(iNaturalist 2018), we set the number of

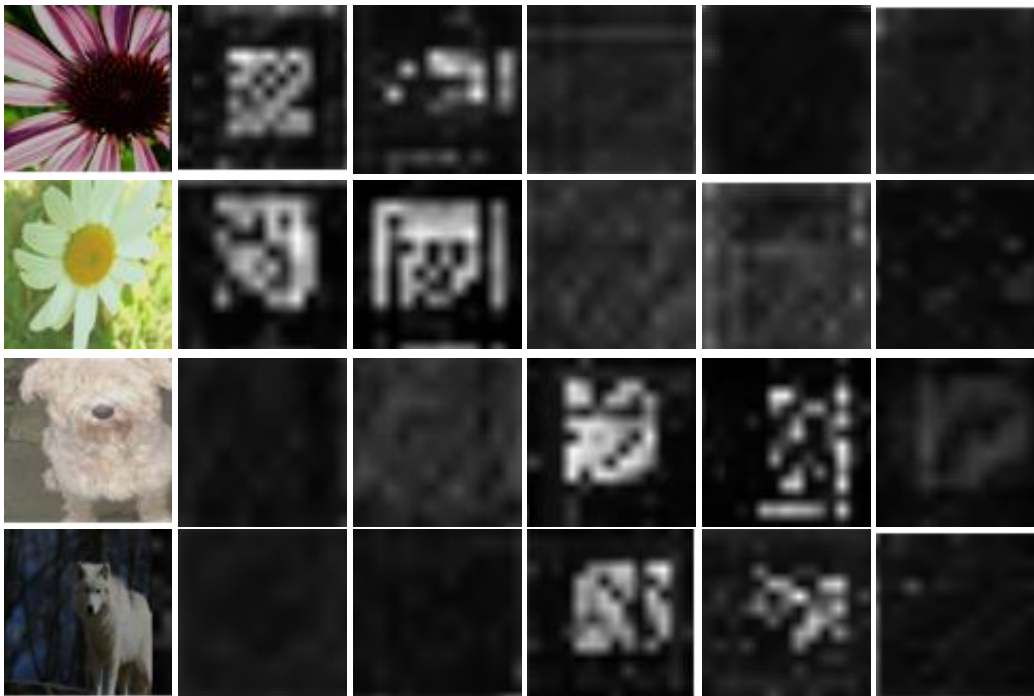


Fig. 5: We visualize the similarity maps generated with latent category features and the image features. As shown in the figures, we randomly select 5 similarity maps from all M similarity maps.

latent categories to 100 with a small training batch size(16) due to resource limitations. As shown in Table III, only adding our proposed latent categories could have a significant improvement over the baseline method for all the datasets. The performances are further improved by applying the latent augmentation loss and the latent reconstruction loss.

Visualization of the latent categories. As shown in Figure 4, we visualize the latent category histogram on the ImageNet-LT dataset with 100 latent categories. We reconstruct the image features with the latent categories, and each latent category contributes with a normalized similarity weight generated by equation 2. As shown in the figure, the 79th latent category (green) is highlighted by the ‘hare’ and ‘dogs’ (Image E and F), while both of them contain similar limb patterns. Furthermore, the ‘cow’, ‘human arm’, and ‘fisher’ also share some commonalities captured by the 98th latent category(red). To be noticed, our proposed method aims to learn some commonalities between the images which belong to the latent classes, not only the appearance from the human perspective. The common features can be any character of the objects, such as the color or the shape. We also visualize the similarity maps in Figure 5.

Latent augmentation vs. ISDA As shown in Table IV, we directly apply the ISDA [14] method to the original class features and conduct the experiments on CIFAR-10-LT and CIFAR-100-LT with different imbalance impacts. Due to the insufficient semantic direction for the tail classes, the performance drops quickly in all the experiment settings. In contrast to directly using the unbalanced features, our latent augmentation method augments the features among the latent categories. It brings significant improvement to all the long-tail

recognition datasets. Specifically, we set the number of latent categories as 40 for CIFAR-10-LT and 50 for CIFAR-100-LT.

V. CONCLUSION

In this paper, we have proposed a latent category-based long-tail recognition(LCReg) method to increase the diversity of the training samples for long-tailed recognition tasks by mining out the common features among the head and tail classes. We adopt a semantic data augmentation method on our proposed latent category features to implicitly enrich the diversity of the training samples. Experiments on several long-tailed recognition benchmarks validate the effectiveness of our method and show our method achieves state-of-the-art performance.

REFERENCES

- [1] O. Russakovsky, J. Deng, H. Su, J. Krause, S. Satheesh, S. Ma, Z. Huang, A. Karpathy, A. Khosla, M. Bernstein *et al.*, “Imagenet large scale visual recognition challenge,” *International journal of computer vision*, vol. 115, no. 3, pp. 211–252, 2015. 1, 6
- [2] M.-E. Nilsback and A. Zisserman, “Automated flower classification over a large number of classes,” in *2008 Sixth Indian Conference on Computer Vision, Graphics & Image Processing*. IEEE, 2008, pp. 722–729. 1
- [3] Y. Wang, D. Ramanan, and M. Hebert, “Learning to model the tail,” in *Advances in Neural Information Processing Systems*, 2017, pp. 7029–7039. 1, 2
- [4] C. Huang, Y. Li, C. C. Loy, and X. Tang, “Deep imbalanced learning for face recognition and attribute prediction,” *IEEE transactions on pattern analysis and machine intelligence*, vol. 42, no. 11, pp. 2781–2794, 2020. 1
- [5] T. Mikolov, I. Sutskever, K. Chen, G. S. Corrado, and J. Dean, “Distributed representations of words and phrases and their compositionality,” *Advances in neural information processing systems*, vol. 26, 2013. 1, 2

- [6] C. Drummond and R. Holte, "C4.5, class imbalance, and cost sensitivity: Why under-sampling beats oversampling," *Proceedings of the ICML'03 Workshop on Learning from Imbalanced Datasets*, 01 2003. 1, 2
- [7] M. Buda, A. Maki, and M. A. Mazurowski, "A systematic study of the class imbalance problem in convolutional neural networks," *Neural Networks*, vol. 106, pp. 249–259, 2018. 1, 2
- [8] L. Shen, Z. Lin, and Q. Huang, "Relay backpropagation for effective learning of deep convolutional neural networks," in *European Conference on Computer Vision*, 2016, pp. 467–482. 1, 2
- [9] N. Sarafianos, X. Xu, and I. A. Kakadiaris, "Deep imbalanced attribute classification using visual attention aggregation," in *European Conference on Computer Vision*, vol. 11215. Springer, 2018, pp. 708–725. 1, 2
- [10] J. Wu, L. Song, Q. Zhang, M. Yang, and J. Yuan, "Forestdet: Large-vocabulary long-tailed object detection and instance segmentation," *IEEE Transactions on Multimedia*, pp. 1–1, 2021. 1
- [11] L. Wang, M. Zhou, Z. Niu, Q. Zhang, and N. Zheng, "Adaptive ladder loss for learning coherent visual-semantic embedding," *IEEE Transactions on Multimedia*, pp. 1–1, 2021. 1
- [12] J. Wang, X. Wang, T. Shen, Y. Wang, L. Li, Y. Tian, H. Yu, L. Chen, J. Xin, X. Wu, N. Zheng, and F.-Y. Wang, "Parallel vision for long-tail regularization: Initial results from ivfc autonomous driving testing," *IEEE Transactions on Intelligent Vehicles*, pp. 1–1, 2022. 1
- [13] L. You, R. Liu, H. Zhang, and Z. M. Shan, "Graph regularized non-negative matrix factorization with long-tail constraint," in *2019 IEEE Pacific Rim Conference on Communications, Computers and Signal Processing (PACRIM)*, 2019, pp. 1–5. 1
- [14] Y. Wang, X. Pan, S. Song, H. Zhang, G. Huang, and C. Wu, "Implicit semantic data augmentation for deep networks," *Advances in Neural Information Processing Systems*, vol. 32, pp. 12 635–12 644, 2019. 1, 3, 4, 5, 6, 8
- [15] S. Li, K. Gong, C. H. Liu, Y. Wang, F. Qiao, and X. Cheng, "Metasaug: Meta semantic augmentation for long-tailed visual recognition," in *Proceedings of the IEEE/CVF Conference on Computer Vision and Pattern Recognition*, 2021, pp. 5212–5221. 1, 3, 6
- [16] W. Liu, C. Zhang, G. Lin, and F. Liu, "Crnet: Cross-reference networks for few-shot segmentation," in *Proceedings of the IEEE/CVF Conference on Computer Vision and Pattern Recognition*, 2020, pp. 4165–4173. 2
- [17] W. Liu, G. Lin, T. Zhang, and Z. Liu, "Guided co-segmentation network for fast video object segmentation," *IEEE Transactions on Circuits and Systems for Video Technology*, 2020. 2
- [18] T. Zhang, G. Lin, W. Liu, J. Cai, and A. Kot, "Splitting vs. merging: Mining object regions with discrepancy and intersection loss for weakly supervised semantic segmentation," in *European Conference on Computer Vision*. Springer, Cham, 2020, pp. 663–679. 2
- [19] W. Liu, C. Zhang, G. Lin, T.-Y. Hung, and C. Miao, "Weakly supervised segmentation with maximum bipartite graph matching," in *Proceedings of the 28th ACM International Conference on Multimedia*, 2020, pp. 2085–2094. 2
- [20] W. Liu, C. Zhang, H. Ding, T.-Y. Hung, and G. Lin, "Few-shot segmentation with optimal transport matching and message flow," *arXiv preprint arXiv:2108.08518*, 2021. 2
- [21] W. Liu, Z. Wu, H. Ding, F. Liu, J. Lin, and G. Lin, "Few-shot segmentation with global and local contrastive learning," *arXiv preprint arXiv:2108.05293*, 2021. 2
- [22] W. Liu, X. Kong, T.-Y. Hung, and G. Lin, "Cross-image region mining with region prototypical network for weakly supervised segmentation," *IEEE Transactions on Multimedia*, 2021. 2
- [23] Z. Wu, X. Shi, G. Lin, and J. Cai, "Learning meta-class memory for few-shot semantic segmentation," in *Proceedings of the IEEE/CVF International Conference on Computer Vision*, 2021, pp. 517–526. 2
- [24] Z. Wu, G. Lin, and J. Cai, "Keypoint based weakly supervised human parsing," *Image and Vision Computing*, vol. 91, p. 103801, 2019. 2
- [25] Z. Wu, Q. Tao, G. Lin, and J. Cai, "Exploring bottom-up and top-down cues with attentive learning for weakly supervised object detection," in *Proceedings of the IEEE/CVF Conference on Computer Vision and Pattern Recognition*, 2020, pp. 12 936–12 945. 2
- [26] Z. Wu, G. Lin, Q. Tao, and J. Cai, "M2e-try on net: Fashion from model to everyone," in *Proceedings of the 27th ACM International Conference on Multimedia*, 2019, pp. 293–301. 2
- [27] X. Zhong, Z. Wu, T. Tan, G. Lin, and Q. Wu, "Mv-ton: Memory-based video virtual try-on network," in *Proceedings of the 29th ACM International Conference on Multimedia*, 2021, pp. 908–916. 2
- [28] A. More, "Survey of resampling techniques for improving classification performance in unbalanced datasets," *CoRR*, vol. abs/1608.06048, 2016. 2
- [29] C. Huang, Y. Li, C. C. Loy, and X. Tang, "Learning deep representation for imbalanced classification," in *IEEE/CVF Conference on Computer Vision and Pattern Recognition*, 2016, pp. 5375–5384. 2
- [30] N. Japkowicz and S. Stephen, "The class imbalance problem: A systematic study," *Intelligent data analysis*, vol. 6, no. 5, pp. 429–449, 2002. 2
- [31] J. Tan, C. Wang, B. Li, Q. Li, W. Ouyang, C. Yin, and J. Yan, "Equalization loss for long-tailed object recognition," in *IEEE/CVF Conference on Computer Vision and Pattern Recognition*. IEEE, 2020, pp. 11 659–11 668. 2
- [32] Z. Zhong, J. Cui, S. Liu, and J. Jia, "Improving calibration for long-tailed recognition," in *Proceedings of the IEEE/CVF Conference on Computer Vision and Pattern Recognition*, 2021, pp. 16 489–16 498. 2, 3, 6, 7
- [33] B. Kang, S. Xie, M. Rohrbach, Z. Yan, A. Gordo, J. Feng, and Y. Kalantidis, "Decoupling representation and classifier for long-tailed recognition," in *International Conference on Learning Representations*, 2020. 2, 3, 5, 6
- [34] K. Tang, J. Huang, and H. Zhang, "Long-tailed classification by keeping the good and removing the bad momentum causal effect," *Advances in neural information processing systems*, vol. 33, 2020. 3, 7
- [35] B. Zhou, Q. Cui, X.-S. Wei, and Z.-M. Chen, "BBN: Bilateral-branch network with cumulative learning for long-tailed visual recognition," in *IEEE/CVF Conference on Computer Vision and Pattern Recognition*, 2020, pp. 9719–9728. 3, 6, 7
- [36] Y. Zhang, X. Wei, B. Zhou, and J. Wu, "Bag of tricks for long-tailed visual recognition with deep convolutional neural networks," in *Association for the Advancement of Artificial Intelligence*, 2021, pp. 3447–3455. 3
- [37] S. Li, M. Xie, K. Gong, C. H. Liu, Y. Wang, and W. Li, "Transferable semantic augmentation for domain adaptation," in *IEEE/CVF Conference on Computer Vision and Pattern Recognition*, 2021, pp. 11 516–11 525. 3
- [38] Z. Liu, Z. Miao, X. Zhan, J. Wang, B. Gong, and S. X. Yu, "Large-scale long-tailed recognition in an open world," in *Proceedings of the IEEE/CVF Conference on Computer Vision and Pattern Recognition*, 2019, pp. 2537–2546. 5, 6, 7
- [39] K. Cao, C. Wei, A. Gaidon, N. Arechiga, and T. Ma, "Learning imbalanced datasets with label-distribution-aware margin loss," *arXiv preprint arXiv:1906.07413*, 2019. 5, 6
- [40] H. Zhang, M. Cisse, Y. N. Dauphin, and D. Lopez-Paz, "mixup: Beyond empirical risk minimization," *International Conference on Learning Representations*, 2018. 6
- [41] K. Cao, C. Wei, A. Gaidon, N. Arechiga, and T. Ma, "Learning imbalanced datasets with label-distribution-aware margin loss," in *Advances in neural information processing systems*, 2019, pp. 1567–1578. 6, 7
- [42] H.-P. Chou, S.-C. Chang, J.-Y. Pan, W. Wei, and D.-C. Juan, "Remix: Rebalanced mixup," in *European Conference on Computer Vision Workshop*, 2020. 6
- [43] T.-Y. Lin, P. Goyal, R. Girshick, K. He, and P. Dollár, "Focal loss for dense object detection," in *International Conference on Computer Vision*, 2017, pp. 2980–2988. 6
- [44] Y. Cui, M. Jia, T.-Y. Lin, Y. Song, and S. Belongie, "Class-balanced loss based on effective number of samples," in *IEEE/CVF Conference on Computer Vision and Pattern Recognition*, 2019, pp. 9268–9277. 6
- [45] X. Zhang, Z. Fang, Y. Wen, Z. Li, and Y. Qiao, "Range loss for deep face recognition with long-tailed training data," in *International Conference on Computer Vision*, 2017, pp. 5409–5418. 7
- [46] S. Gidaris and N. Komodakis, "Dynamic few-shot visual learning without forgetting," in *IEEE/CVF Conference on Computer Vision and Pattern Recognition*, 2018, pp. 4367–4375. 7
- [47] L. Xiang and G. Ding, "Learning from multiple experts: Self-paced knowledge distillation for long-tailed classification," in *European Conference on Computer Vision*, 2020. 7
- [48] G. Van Horn, O. Mac Aodha, Y. Song, Y. Cui, C. Sun, A. Shepard, H. Adam, P. Perona, and S. Belongie, "The iNaturalist species classification and detection dataset," in *IEEE/CVF Conference on Computer Vision and Pattern Recognition*, 2018, pp. 8769–8778. 6
- [49] B. Zhou, A. Lapedriza, A. Khosla, A. Oliva, and A. Torralba, "Places: A 10 million image database for scene recognition," *IEEE Transactions on Pattern Analysis and Machine Intelligence*, vol. 40, no. 6, pp. 1452–1464, 2017. 7